UNIVERSITY OF CALIFORNIA,

IRVINE

Construction of Fluorescence Lifetime Silica Nanoprobe Library with Tunable Lifetime Properties

THESIS

submitted in partial satisfaction of the requirements

for the degree of

MASTER OF SCIENCE

in Biomedical Engineering

by

Xi Chen

Thesis Committee:
Assistant Professor Jered B. Haun, Chair
Assistant Professor Michelle A. Digman
Associate Professor James P. Brody

2019

TABLE OF CONTENTS

LIST OF FIGURES

ACKNOWLEDGEMENTS

Here, I would like to express my sincere thanks to Professor Jered Haun for giving me the chance to join this perfect lab and providing me the opportunity to investigate this meaningful project I would not finish this work without his belief in me. Moreover, Prof. Haun's continuous support also helped me overcome the difficulties during doing my research. I also would like to express my thanks to my committee members, Professor Digman and Professor Brody, for their guidance on my dissertation and their valuable time.

Also, I would like to show my acknowledgements towards Louis Mejia for all his helps. He taught me not only the knowledge need for doing my research with all his patience, he also shared his experiments and life experience with me without holding back, which really helps me going through hard times. Additionally, I would like to express my thanks to Maha, Jinghui, Hauna and other lab members for their supports, accompany and guidance. They formed a great lab culture that makes me enjoy every minutes in the lab.

Last but not least, I would like to express my gratitude towards my family for their love. Their unconditional support gives me the chance to pursue my dreams.

ABSTRACT OF THE THESIS

Construction of Fluorescence Lifetime Silica Nanoprobe Library with Tunable Lifetime Properties

By

Xi Chen

Master of Science in Biomedical Engineering

University of California, Irvine, 2019

Assistant Professor Jered B. Haun, Chair

Tumor heterogeneity means the ecosystem of tumor contains variety of cell types, which makes cancer cells hard to detect and increases the difficulty of cancer treatment. Fluorescent probes can provide the molecular information that is critical for diagnosis. The range of fluorescence emission within the visible spectrum allows for multiple target labels. However, a limited range of fluorescence probes have been synthesized and are available for use. Therefore, expanding the number of probes becomes an urgent task. Fluorescence lifetime imaging microscopy (FLIM) can identify fluorescent species based solely on the fluorescence lifetime. The phasor approach to FLIM graphically depict lifetime distributions on a pixel-by-pixel basis. So, the phasor approach to FLIM could be an effective tool in helping to boost the number of detection channels if a library of lifetime probes could be constructed. In addition, the tunability of fluorescent lifetimes can be graphically represented on the phasor plot by determining the fractional contribution of two

fluorescent probes. Thus, the main idea of this study is to construct libraries of probes with unique fluorescent lifetimes that will increase the detection capacity of fluorescence imaging. In this study, new fluorescent probes were made by encapsulating different fluorescent species inside the silica nanoparticles through reverse microemulsion methods. Three kinds of lifetime probe mixtures have been synthesized by encapsulating different types of quantum dots, both quantum dots and dark quencher dyes, and quantum dots and fluorescent dyes inside the silica nanoparticles. By changing the amount of fluorescent species, tunable fluorescent lifetime can be achieved. The first fluorescent lifetime libraries have been constructed by synthesizing the probes with different fluorescent species and then selecting the ideal lifetimes. The construction and expansion of fluorescent lifetime probe libraries provides a possibility of simultaneously detecting multiple targeted cell types.

Chapter 1 Introduction

1.1 Cancer Detection

According to the annual report of cancer last year, the overall cancer death rates in the U.S. continue to decrease [1]. In order to reduce the cancer death rate, improvement methods for early diagnosis ability is required. However, tumor infiltration and metastasis increase the tumor heterogeneity, and makes them more difficult to detect.

Tumor heterogeneity usually includes two types, inter-tumor heterogeneity and intra-tumor heterogeneity, which emphasize the variation of cells that occurred between different cells or within the same cell, respectively [2]. So, various types of cells have been derived. Key cell types, like those arising from cancer stem cells (CSCs) that experience the process of hierarchical differentiation, require fast identification before the effective treatment can be implemented. Thus, efficient detection methods need to be developed.

A lot of molecular detection techniques have already been implemented in research use or even clinical use. For instance, next generation sequencing can determine gene mutations that happen in KRAS, BRAF and EGFR [3, 4]. However, the detection ability of these methods has been hindered by problems such as the artifacts in detection process may affect the results, or testing where expends all the samples, and thus limits the possibility for further testing.

Molecular probe is an alternative platform that can provide molecular information such as the

expression level and location of cells. Non-fluorescent probe platforms such as surface-enhanced Raman scattering (SERS) and mass cytometry have been well developed. SERS is a technique that enhances Raman scattering through the coupling of molecules and rough metal surfaces and nanoparticles induced by the absorption function [5, 6]. However, a unified theory of SERS which can take advantage of both physical and chemical enhancement mechanisms has not yet to be found. Another problem of SERS is due to the problems encountered within the experiment, such as local heating. These two issues have together blocked the development of SERS in detection use. Mass cytometry is a technique based on inductively coupled plasma mass spectrometry and is used to determine time-of-flight mass spectrometry for cell characteristics [7]. With the help of those isotope-labeled antibodies, proteins are eventually labeled. Nevertheless, the relative low scanning speed makes it less user friendly and cause low testing efficiency. Thus, this method fail to meet the requirements for high throughput testing.

Fluorescent molecular probes are often used in molecular detection platforms like fluorescent imaging microscopy or fluorescent spectrometry [8]. With the use of fluorescent probes, molecular information like concentration, expression level, location in cells can be obtained. Moreover, as more probes are used at the same time, quick and simultaneously multiplexed detection can be implemented. However, the great potential of fluorescent molecular probes in fluorescent imaging has not been achieved because only limited numbers of probes are available. Thus, there is a need to develop more probes, and thereby enrich the efficiency of fluorescent molecular probes for detection.

1.2 The Phasor Approach to FLIM

Fluorescence lifetime refers to the average residence time of a molecule before it returns to the ground state after being excited by a light pulse. Fluorescence lifetime imaging microscopy (FLIM) can calculate the fluorescence lifetime of samples voxel by voxel and form images to reflect the distribution of fluorescent substances in cells [9, 10]. However, most organic fluorescent species have similar lifetimes which cannot be distinguished by FLIM.

In recent years, with the development of the phasor approach to FLIM, great progress has been made in fluorescent lifetime analysis [11]. The phasor approach can convert the lifetime attenuation data into frequency domain and make the results visible on phasor plot.

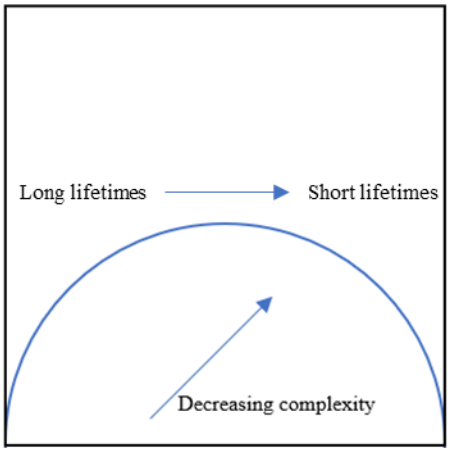

Figure 1.1 The phasor plot shows the lifetime decay trend and the complexity.

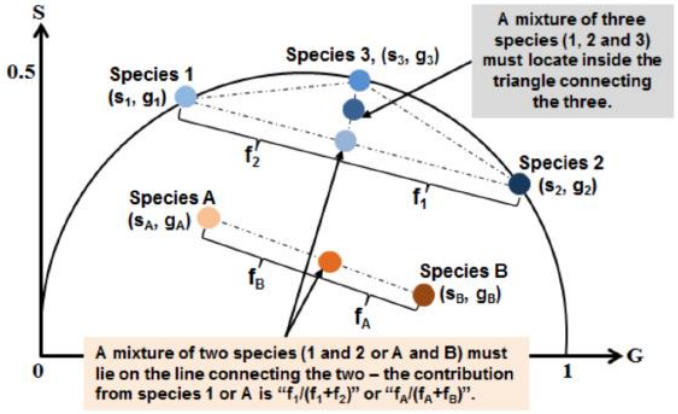

Figure 1.2 Linear decomposition of multiple species. [12]

While the phasor plot can directly present the lifetime of single-lifetime species, for the mixture of two or more species, its lifetime is decomposed as a linear combination of those species (Figure 1.2). In addition, with the using of the phasor approach to FLIM, species that have similar emission spectra can be located on completely different spots on the phasor plot due to their difference in intrinsic fluorescence lifetime.

So, we would like to use FLIM to construct fluorescent lifetime probe library that could achieve simple and quick molecular detection by employing different fluorescent species in the probe making process.

1.3 Project Overview

As molecular probes have been considered a tool for cancer cells detection that can providing enough information needed, it is meaningful to develop more probes. However, current probe

detection platforms exhibit shortcomings like they are hard to use and cannot detect many channels at the same time. The phasor approach to FLIM makes huge advance as lifetime decay information can be directly seen on phasor plot. However, as only limited number of probes have been developed, the potential of FLIM also doesn't be fully presented. Thus, this study mainly focused on making fluorescence probe lifetime library by incorporate different fluorescent species with various amount of doped. By using this library, quick and high throughput detection can be conducted.

First, this study presented how silica nanoparticle probes were synthesized with reverse microemulsion method. Then, as three kinds of fluorescent species are widely used nowadays, the next three chapters described how the lifetime library was constructed by mixed them with each other within the single silica nanoparticles. The lifetime libraries are classified into quantum dot and quantum dot mixed probe libraries, quantum dot and dark quencher dye mixed probe libraries, and quantum dot and fluorescent dye mixed probe libraries. During the synthesis process, different species are encapsulated inside the silica nanoparticles for making specific probes, in addition, species concentration also is optimized in order to tune lifetime. Particle size, absorption and emission intensities, and FLIM phasor location for all probes are measured for characterization of the developed probes. Finally, after all characterizations are finished, their phasor locations are tested and used to construct the global probe lifetime libraries.

Chapter 2 Synthesis and Characterization of Silica Nanoparticle Probes

2.1 Silica Nanoparticles

The particles with nanosized diameter are called nanoparticles [13]. Nanoparticles are often used for fluorescent biological labeling and pathogen detection. The material of nanoparticles used in biology field often contains gold, silver, magnetite and silica. Among all these materials, the widely detection-used nanoprobes are made by silica nanoparticles. The silica nanoparticles have rather low cellular toxicity than other materials [14]. Meanwhile, it also has tunable particle size and high surface area [15]. Besides, the surface is easy to be modified, thus after connecting to specific groups, it can conjugate with antibodies. Thus, currently silica nanoparticles have been intensively investigated in materials research.

As silica nanoparticle have been decided to be employed, the exact nanoprobes that used are based on the modification of general silica nanoparticles. In the next few chapters, composite fluorescent silica nanoparticles are sought to be synthesized and tested.

Fluorescent silica nanoparticles are a new type of silica nanoparticles with obvious core-shell structure, which are usually composed by fluorescent materials in the core and silica shell that could be modified [16]. With the protection of silica shell, fluorescent species can have lower toxicity to cells and avoid photobleaching while still maintain high fluorescent intensity [17, 18].

Fluorescent species, such as quantum dots, fluorescent dyes, rare earth luminescent materials can all be incorporated into the silica nanoparticles. Organic dyes that doped inside the silica nanoparticles have been showed of having many advantages and already put into real world [19]. As these fluorophores are doped inside the silica nanoparticle shell, they can be well-protected from the environment [20]. Then, nanoparticles that having different functional groups on the surface can be prepared using different chemical reagents. Thus, they can covalently bind with antibodies or immobilized with other kind of biomolecules for future detection use.

2.2 Synthesis of Silica Nanoparticles (SNPs) by Reverse Microemulsion Method

Nowadays, there are many kinds of methods that can be used to synthesis silica nanoparticle, StÖber method, hydrothermal method, microemulsion method and reverse microemulsion method. With these methods, silica nanoparticles with tunable size can be produced. From the reason above also based on the previous study, the exact method that used by Haun group and in this study is an updated version of reverse microemulsion method [21]. Emulsion droplet template should be created first to trigger the nucleation. Thus, 1.3mL of IGEPAL CO-520 surfactant was added into the 10mL of cyclohexane to create the water in oil droplet. Sonicate until clear.

Next, as the water in oil emulsion droplets are formed, quantum dots could be added. Then, sonicate for 5 minutes in order to let quantum dots be well-disperse in droplets that have been created before. Thus, after all procedures are finished, quantum dots can stay inside the droplet

and then embedded on the silica mesh.

After adding quantum dots, dark quencher dyes or fluorescent dyes could be encapsulated, too. In order to encapsulate dyes successfully inside the silica nanoparticles, pretreatment must be done before use. Those dyes were bought with N-Hydroxysuccinimide-ester (NHS) group. So, $-NH_2$ group on APTS can react with NHS group. Then, with the reaction between the other three ethoxy group on APTS and the ethoxy group on TEOS, dyes can get involved into the nucleation process. Finally, they are encapsulated inside the silica cores.

After 5 minutes sonication, 150 μL of ammonia is added to provide both water and alkaline environment for the hydrolysis and condensation of tetraethyl orthosilicate (TEOS) and thus form droplet interior. Then, sonicate for 1 minute and add 80 μL of TEOS. Now, the silica source has been provided. After 24 hours, silica nanoparticle cores should be produced.

2.3 Surface Modification

After encapsulating the quantum dots and dark quencher dyes inside the silica particle cores, we still want to modify the surface of silica nanoparticle cores to ensure that we can further use the SNPs as an effective probe to target the antibodies. This means there are still several procedures need to be done. This time, 2μL of carboxyethylsilanetriol and 1 μL of 3-(trihydroxysilyl)propyl methylphosphonate were added. While phosphonate silane can help silica nanoparticles being more dispersed rather than aggregate together, carboxylic acid can be used for future binding with

antibodies.

Finally, again after 24 hours, we will wash the particles to remove the unreacted materials. The process would be that transfer 1mL of solution and 0.5 mL of ethanol into the Eppendorf centrifuge tube, after centrifuging it for 15 min at 11,500 rcf, dispose supernatant. Then, add 1 mL of ethanol into this centrifuge tube and repeat centrifuging for two times. In the end, add 1 mL of water into the centrifuge tube to make it as an aqueous solution that can be used for testament.

2.4 Characterization Methods

2.4.1 Fluorescence Lifetime

The fluorescence lifetime imaging data was gathered by a highly customized Olympus FluoView FV1000 instruments with ISS A320 FastFLIM one-photon data acquisition card. The microscope used was IX81 with UPLSAPO 60X objective lens. The emission detection range was between 560 to 660nm. The excitation wavelength was set to 488/543/633 nm.

2.4.2 Emission and Absorption

Cary-60 absorption spectrometer and Cary Eclipse fluorimeter that from Agilent are used to test absorption and emission intensities. As required by instruments, additional 1.5 mL of water should be added to fulfill the instruments requirements. For absorption, the range reading was set to 200nm to 800nm wavelength. as the absorption spectra of silica showed up around 250nm to 350nm, the absorption intensity was picked at 300nm. For emission settings, the range recorded

was from 500nm to 750nm wavelength. As emission intensity varies a lot from each kind of fluorescent species, the voltage used were always adjust according to the actual condition. The emission wavelength was picked in which the highest intensity occurred.

2.4.3 Size

Information about the size of particles are provided using the dynamic light scattering through Malven Zetasizer Nano DLS instrument. As the samples are already in 1 mL of water, measurement can directly conduct.

Chapter 3 Construction of Lifetime Library: Silica Nanoparticles with Different Quantum Dots

3.1 Quantum Dots

Quantum dots (QD), as a kind of semiconductor nanocrystal materials, have advantages like size-tunable narrow emission spectral, broad absorbance, and also do not have significant photobleach phenomenon [22, 23]. QD have been highly applied in the biology field. Through bioconjugation, it further showed its ability in molecular labelling, fluorescence imaging, etc. [24]. For instance, proteins that with polyhistidine can self-assembled to quantum dots [25] So, having quantum dots encapsulated in our silica nanoparticles would be a benefit because the nanoprobe we made will eventually conjugate to antibodies and then detect cancer cells. By adjust to various kinds of quantum dots, multiple probes with unique fluorescent lifetime can be obtained.

Quantum dots inside the silica nanoparticles can generate quenching effect with other quantum dots or fluorescent species. By using quantum dots and then letting other fluorescent materials arrange around it can control the fluorescent lifetime. [26, 27, 28]. Thus, through the adjustment of materials doped inside the silica nanoparticles, multiple locations on the phasor plot can be achieved.

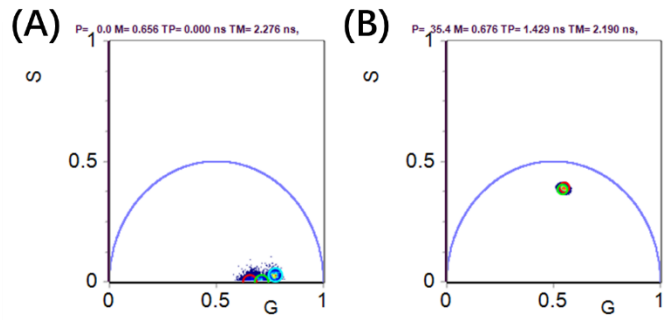

Figure 3.1: Comparision between two quantum dots structures. Silica nanoparticles labeled with quantum dots from Strem company with (A) CdSe core only, (B) CdSe/CdS core/shell structure, water as the solvent.

The quantum dots are usually sold with two kinds of structures, core only, and core/shell structure. Quantum dots brought from Strem company with these two structures were tested before (Figure 3.1). From the FLIM results, quantum without protection of shell have bad manners on the phasor plot, as the lifetime quenched a lot and dimmer than quantum dots with core/shell structure, which also indicate they have lower emission intensity. So, the quantum dots that we employed always have the core/shell structure.

In order to help future study of molecular expression level analyzation, for normalization, all fluorescent species (quantum dots and quencher dyes in this chapter, and fluorescent dyes in the next chapter) we employed in this research have the similar emission wavelength (570-600 nm). However, as they have distinct lifetimes, they will still occupy different place on the FLIM phasor plot after encapsulated inside the silica nanoparticles.

3.2 Materials and Methods

In this part of study, four different quantum dots were used to construct unique fluorescent lifetime

probes by doping them inside the silica nanoparticles. Here, quantum dots employed were CZ (CdSe/ZnS), CIS (CuInS/ZnS), InP (InP/ZnS) from NN-Labs, and quantum rods from Strem (CdSe/CdS) company. In order to find the probe that not only have unique lifetime, high fluorescent intensity, but also stable to be used, different quantum dots concentration was tested. According to the intrinsic properties of quantum dots products, the concentration of CZ was set to 20, 50, 100 and 200 μL, Strem was 50, 75, 100 and 150 μL, CIS for 30, 50, 100, 150 and 200 μL, and InP for 50, 100, 150 and 200 μL.

Then, in order to enrich the number of usable nanoprobes, the effect on lifetime information of mixing two different quantum dots were also tested. Thus, silica nanoparticles that doped with CZ and Strem in the ratio of 100 μL CZ and 100 μL Strem (1:1), 150 μL CZ and 50 μL Strem (3:1), 50 μL CZ and 150 μL Strem (1:3) were made.

3.3 Characterization Results

3.3.1 Fluorescence Lifetime

First, phasor plot information of CZ, Strem, CIS and InP alone inside the silica nanoparticles were demonstrated by FLIM, respectively. From the results, Strem have the shortest lifetime than other three kinds of quantum dots. Also, CZ and Strem are more stable to use than CIS and InP because that with the concentration increased, their lifetime is approximately the same. While at the same time, the lifetime of CIS and InP keep changing along with the concentration increased. At low concentration, the FLIM results of silica nanoparticles with CIS and InP displayed themselves as

a dim and noisy circle on the phasor plot, and with the amount of used increased, they become brighter and centered as a smaller circle. These results showed that CZ and Strem are more concentrated and also brighter than CIS and InP, but still not reach the degree that would cause quantum dots homo-quenching effect.

(A)

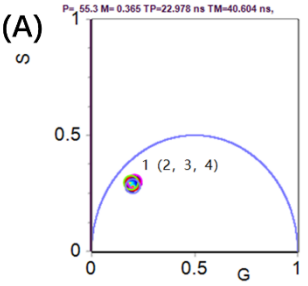

	Color	QDs	Conc (μL)	DLS (nm)	Emission (350 ex, 597 nm)	Absorption (300 nm)	Emission / Absorption
1	Red	CZ	20	40.12	0.0364	0.1653	0.2204
2	Yellow	CZ	50	43.41	0.1552	0.2015	0.7700
3	Green	CZ	100	43.39	0.3986	0.2645	1.5067
4	Pink	CZ	200	36.72	0.7385	0.3417	2.1613

(B)

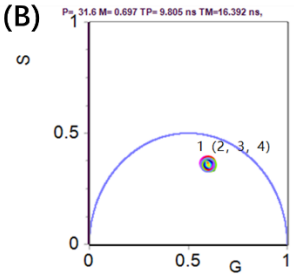

	Color	QDs	Conc (μL)	DLS (nm)	Emission (350 ex, 593 nm)	Absorption (300 nm)	Emission / Absorption
1	Red	Strem	50	36.79	0.3829	0.3163	1.2107
2	Yellow	Strem	75	35.10	0.3485	0.3279	1.0630
3	Green	Strem	100	43.08	0.6401	0.5128	1.2482
4	Pink	Strem	150	38.42	0.6944	0.4948	1.4035

(C)

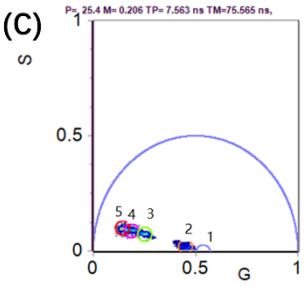

	Color	QDs	Conc (μL)	DLS (nm)	Emission (350 ex, 582 nm)	Absorption (300 nm)	Emission / Absorption
1	Purple	CIS	30	43.02	0.0529	0.1614	0.3279
2	Orange	CIS	50	48.21	0.1143	0.1928	0.5928
3	Green	CIS	100	51.53	0.3334	0.2391	1.3948
4	Pink	CIS	150	59.37	0.4903	0.3144	1.5591
5	Red	CIS	200	49.92	0.7734	0.3040	2.5441

(D)

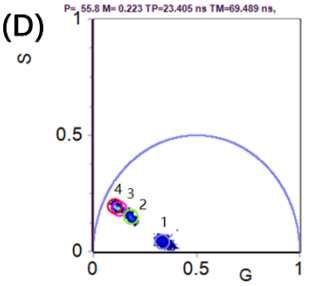

	Color	QDs	Conc (μL)	DLS (nm)	Emission (350 ex, 580 nm)	Absorption (300 nm)	Emission / Absorption
1	Purple	InP	50	47.42	0.0495	0.2490	0.1986
2	Green	InP	100	42.24	0.1796	0.4207	0.4269
3	Pink	InP	150	47.28	0.5388	0.3837	1.4044
4	Red	InP	200	43.34	0.8772	0.4697	1.8673

Figure 3.2 Characterization results of silica nanoparticles labeled with different quantum dots: (A) CZ, (B) Strem, (C) CIS and (D) InP. (Left) Fluorescence lifetime data. (Right) DLS results and intensity readings of emission and absorption of each probe.

Next, to unlock more probes that with different lifetimes, whether two quantum dots mixtures can become effective probes are also interested. So, CZ and Strem mixed probes were tested. When CZ and Strem used in 1:1 ratio, mixed probes locate on the line that in between these two species. This followed the expected quenching trajectory. At the meantime, it was also located near the center of this line. This indicated that the contributions of both species are almost the same. When switched to 3:1 ratio and 1:3 ratio, they still locate on the same line, and the exact location is proportional to 3:1 and 1:3 ratio. All these results again show that in this part of study, the main factor that decided the quenching efficiency was the concentration of quantum dots in the silica nanoparticles.

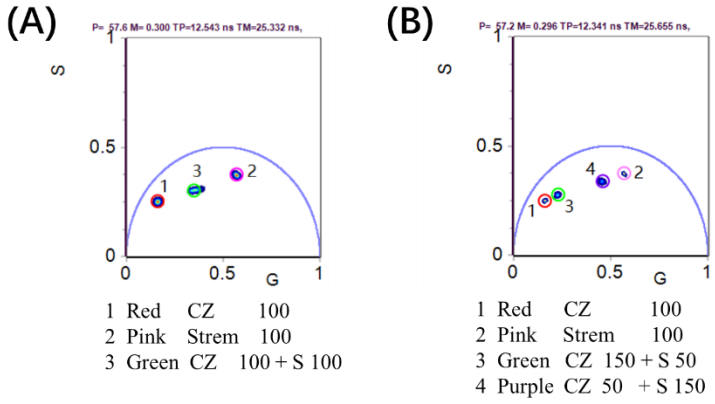

Figure 3.3 FLIM results of QDs-QDs mixed probes. (A) Results of CZ and Strem quantum dots, with 1:1 ratio of amount used. (B) Results of CZ and Strem quantum dots, with 3:1 and 1:3 ratio of amount used.

3.3.2 Fluorescence Analysis

Fluorescence analysis recorded the emission intensity and absorption intensity of four quantum

dots. As the concentration of quantum dots increases, the emission and absorption intensity of all four probes also increase. Thus, the overall fluorescent intensities which is defined by emission intensity over absorption intensity shows a growing trend. This indicate that quantum dots have been successfully incorporated inside the silica matrix, and the fluorescent intensities are shown as quantum dots concentration dependent.

The emission data were acquired after changing settings each time. For CZ, the photomultiplier tube (PMT) voltage was set to 600 volts, for Strem, it increased to 650 volts. While testing the InP and CIS, not only the PMT voltage was changed, but also the emission slit width was increased. The settings for InP is 20 nm emission slit width and 600 volts PMT voltage. For CIS, it was 20 nm emission slit width and 650 volts PMT voltage. So, it can be concluded that CZ and Strem are much brighter than CIS and InP, which matches the FLIM results that CIS and InP shows dimmer and noisy circle on phasor plot, while CZ and Strem are more concentrated. Thus, in the future, CZ and Strem, maybe also along with CIS, are easier and more meaningful to use.

3.3.3 Size

When only have quantum dots encapsulated inside the silica nanoparticles, DLS gave the size of nanoprobes between 40 to 50 nm. This means that when changing the loading of quantum dots, the overall results will not change, which further indicate that our results are reliable, and the probes are effective to be used.

3.4 Fluorescent Lifetime Nanoprobe Library in this Chapter

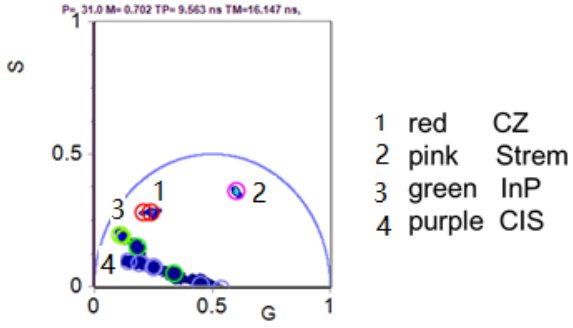

Figure 3.4 Global fluorescent lifetime results of the silica nanoparticles that labeled with four kinds of quantum dots, CZ, Strem, CIS and InP in various concentrations.

Chapter 4 Construction of Lifetime Library: Silica Nanoparticles with Quantum Dots and Dark Quencher Dyes

4.1 Dark Quencher Dye

To enrich the nanoparticle probe library, dark quencher dyes are incorporated to shorten the fluorescence lifetime of quantum dots. When excited dark quencher dyes go back to ground state, intrinsic fluorescence of dark quenchers can be negligible because it emits energy in the format of heat [29, 30]. So, quenching effect that caused by dark quencher can be an effective tool in shortening and tuning the fluorescent lifetime of quantum dot. In this way, dark quenchers were believed can unlock more location on phasor plot.

4.2 Encapsulation

In this part of study, dark quencher dyes with quantum dots are together encapsulated into the silica cores. Dark quencher dye that being used in this portion of study is QXL 570 from AnaSpec which has the emission wavelength around 578 nm.

In the first part, to obtain the trajectory of single type of quantum dots along with dark quencher dyes, three kinds of quantum dots that employed are CZ (CdSe/ZnS), CIS (CuInS/ZnS), InP (InP/ZnS) from NN-Labs, and quantum rods from Strem (CdSe/CdS) company. The amount used in synthesis was set to 200 μL of CZ, 200 & 100 μL of CIS, 200 μL of InP, and 100 μL of Strem. Then, to filling more place on phasor plot, dark quencher dyes also added to CZ-Strem mixtures

of 1:1 ratio and 3:1 ratio that have been made in the previous chapter.

4.3 Characterization Results

4.3.1 Fluorescence Lifetime

From FLIM results, all probes that contain quantum dots only have different fluorescence lifetime, so they start from unique spot on the phasor plot. After adding increased amount of dark quencher dyes, their fluorescence lifetime shortening as expected. While the quenching trajectory of CZ and Strem probes fit the curve of the circle, InP and CIS quenched more horizontally. For silica nanoparticles that contains CZ with dark quencher dyes and Strem with dark quencher dyes, the average radius to the center of semi-circle is almost the same, that means they have the same exponential information and so the complexity of the particles are the same.

Still from the phasor plot, 100 and 200 μL CIS that without dark quenchers are at the same spot. From previous test, CZ, Strem and InP also have the same situation with 100 and 200 μL amount used. The reason is that fluorophores doped inside the particles are not close enough to each other. So, self-quenching did not happen. TEM results valid this explanation, only when 200 μL CZ, 200 μL Strem are encapsulated, situation of one quantum dot inside one single silica nanoparticle can be achieved. For CIS and InP, more than 200 μL should be used to achieve similar degree.

(A)

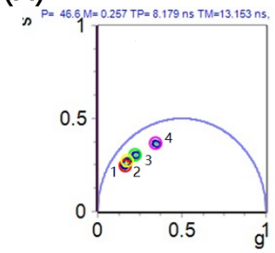

	Color	QDs	Conc (μL)	Quencher (μL)	DLS (nm)	Emission (350 ex, 598 nm)	Absorption (300 nm)	Emission / Absorption
1	Red	CZ	200	0	40.33	0.8425	0.4823	1.7469
2	Yellow	CZ	200	10	41.45	0.2827	0.4472	0.6322
3	Green	CZ	200	30	40.22	0.5469	0.4784	1.1433
4	Pink	CZ	200	60	44.80	0.2663	0.5451	0.4885

(B)

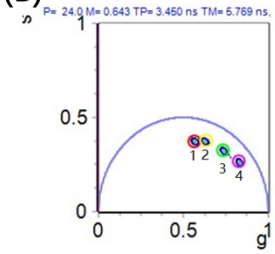

	Color	QDs	Conc (μL)	Quencher (μL)	DLS (nm)	Emission (350 ex, 592 nm)	Absorption (300 nm)	Emission / Absorption
1	Red	Strem	100	0	46.00	0.9563	0.5428	1.7617
2	Yellow	Strem	100	10	52.60	0.5451	0.5602	0.9731
3	Green	Strem	100	30	46.89	0.3388	0.5806	0.5836
4	Pink	Strem	100	60	56.45	0.1725	0.6611	0.2609

(C)

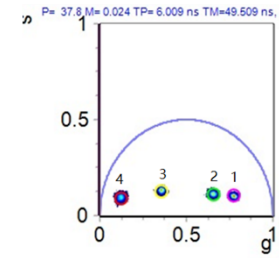

	Color	QDs	Conc (μL)	Quencher (μL)	DLS (nm)	Emission (350 ex, 584 nm)	Absorption (300 nm)	Emission / Absorption
1	Pink	CIS	200	0	47.91	0.6853	0.2679	2.5582
2	Green	CIS	200	10	72.94	0.2033	0.3647	0.5574
3	Yellow	CIS	200	30	51.64	0.0401	0.3466	0.1156
4	Red	CIS	200	60	82.11	0.0335	0.5824	0.0575

(D)

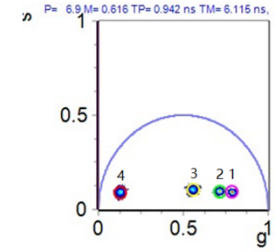

	Color	QDs	Conc (μL)	Quencher (μL)	DLS (nm)	Emission (350 ex, 584 nm)	Absorption (300 nm)	Emission / Absorption
1	Pink	CIS	100	0	52.43	0.2987	0.2134	1.4002
2	Green	CIS	100	10	47.22	0.0571	0.2103	0.2714
3	Yellow	CIS	100	30	56.09	0.0361	0.2996	0.1204
4	Red	CIS	100	60	64.77	0.0178	0.3709	0.0481

Figure 4.1 Characterization results of silica nanoparticles labeled with different quantum dots and QXL 570 dark quencher dyes: (A) 200 μL CZ, (B) 100 μL Strem, (C) 200 μL CIS and (D) 100 μL CIS. (Left) Fluorescence lifetime data that under 470nm excitation wavelength. (Right) DLS results and intensity readings of emission and absorption of each probe.

The lifetime decay data match the fluorescence analysis. For CZ and Strem, when adding 10, 30 and 60 µL of quenchers, the lifetime decay is proportionally to the amount of dyes added. However, for InP and CIS, the decay of lifetime happens more easily. When adding 10, 30 and 60 µL of dark quenchers this time, their lifetime can change to very short. Thus, 1 and 3µL situation are involved to fill the spot in between.

(A)

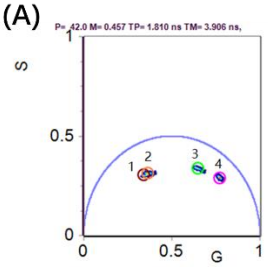

	Color	CZ (µL)	Strem (µL)	Quencher (µL)	DLS (nm)	Emission (350 ex, 597 nm)	Absorption (300 nm)	Emission / Absorption
1	Red	100	100	0	39.09	0.4117	0.7863	0.5236
2	Orange	100	100	10	41.73	0.3394	0.8504	0.3991
3	Green	100	100	30	36.14	0.1195	0.8572	0.1394
4	Pink	100	100	60	57.53	0.0525	1.0519	0.0499

(B)

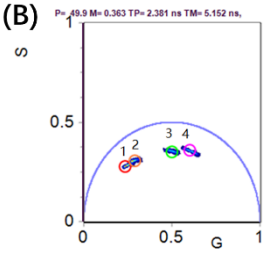

	Color	CZ (µL)	Strem (µL)	Quencher (µL)	DLS (nm)	Emission (350 ex, 597 nm)	Absorption (300 nm)	Emission / Absorption
1	Red	150	50	0	44.38	0.7439	0.7784	0.9558
2	Orange	150	50	10	43.90	0.3431	0.8084	0.4245
3	Green	150	50	30	42.27	0.2023	0.8125	0.2490
4	Pink	150	50	60	43.79	0.0826	0.8979	0.0920

Figure 4.2 Characterization results of CZ and Strem mixed probes with QXL 570 dark quencher dyes: (A) CZ and Strem in 1:1 ratio, (B) CZ and Strem in 3:1 ratio. (Left) Fluorescence lifetime data that under 470nm excitation wavelength. (Right) DLS results and intensity readings of emission and absorption of each probe.

Next, as CZ and Strem mixed probes have already been made in the previous chapter, 1:1 ratio and 3:1 ratio was picked to exam the change of lifetime with the presence of dark quencher dyes. This time, with more dark quencher dyes were incorporated, the level of quenching increased so cause the decrease in fluorescent lifetime.

4.3.2 Fluorescence Analysis

Fluorescence analysis results are recorded for the situations that silica nanoparticles that labeled with quantum dots only, both quantum dots with dark quencher dyes, and CZ-Strem mixed probes with dark quencher dyes. From the data, emission and absorption intensities are shown as dark quencher concentration dependent. Absorption intensities strengthened while the concentration of dark quencher dyes increased, which shows the quantum dot and dye are both inside the silica matrix. While at the meantime, the emission data tells a different story. When dark quencher dyes were incorporated, the interaction between quantum dots and dark quenchers induces quenching effect, so, emission intensities are weakened. Thus, the overall quantum efficiency also decreased. This trend of decrease is inverse proportion to dark quencher dye amount ratio. For 10 μL and 30 μL of dark quencher dye used, their emission intensity over absorption is in the ratio of about 3:1.

4.3.3 Size

From DLS results, majority particles have the size around 40nm. However, as increasing amount of dark quencher dyes are get involved into the synthesis, the diameter of samples also increased a lot. Size of samples that include CZ increased form 40nm to 45nm, Strem and InP increased from 45nm to 55nm, while for CIS with dark quenchers, average diameter changed a lot from 50nm to around 80nm. While for CZ and Strem mixed probes, this tendency of increasing in size also happened, but still in the normal range. This is understandable as more dark quencher dyes are doped, they are getting more and more involved into the silica nucleation process by covalently incorporated into the particle interior.

4.4 Fluorescent Lifetime Nanoprobe Library in this Chapter

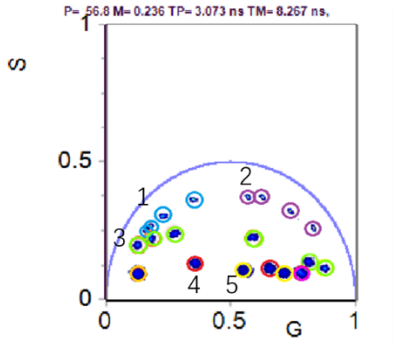

1 Blue CZ 200 µL
2 Purple Strem 100 µL
3 Green InP 200 µL
4 Red CIS 200 µL
5 Orange CIS 100 µL

Figure 4.3: Global fluorescent lifetime results of silica nanoparticles that labeled with three types of quantum dots with different amount of QXL 570 dark quencher dyes, under 470 nm excitation.

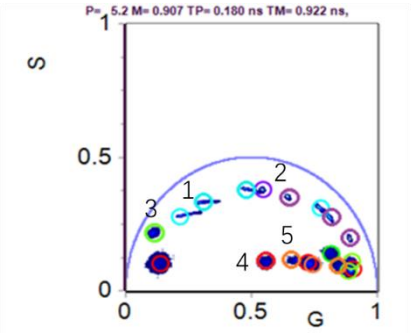

1 Blue CZ 200 µL
2 Purple Strem 100 µL
3 Green InP 200 µL
4 Red CIS 200 µL
5 Orange CIS 100 µL

Figure 4.4: Global fluorescent lifetime results of silica nanoparticles that labeled with three types of quantum dots with different amount of QXL 610 dark quencher dyes, under 470 nm excitation.

The data of same kinds of quantum dots coupled with QXL 610 dyes (also from AnaSpec) in the same ratio are also available. The Haun group used to use QXL 610 dark quencher dyes in research. However, as AnaSpec deciding the termination of QXL 610 production, QXL 570 were employed in the study. After comparing the results between quantum dots with QXL 570 and QXL 610 dyes, it is happy to say that most places that are achieved by QXL 610 can be reproduced by QXL 570. After studying the quenching trajectory of Strem with different amount of quencher dyes, even the most unique position, 100 µL of Strem with 60 µL of QXL 610, can be reproduced by 100 µL of Strem with 80 µL of QXL 570.

Chapter 5 Construction of Lifetime Library: Silica Nanoparticles with Quantum Dots and Fluorescent Dyes

5.1 Fluorescent dyes

After making quantum dots and quantum dots mixed probes and quantum dots with dark quencher dyes mixtures, respectively, we are seeking about employee more fluorescent species in our library construction process.

Different with dark quencher dyes, fluorescent dyes are a kind of materials that can emit light in visible region when going back to the ground state [31]. Thus, their intensive fluorescence made them commonly used in biology detection. For instance, widely used fluorescent dye, rhodamine, can be modified to TMR for which could be used as a fluorescent probe for phagocytosis detection [32]. As all fluorescent species used in this whole study have the absorption wavelength over 550nm, long-wavelength Alexa Fluor dyes are also very useful because they have advantage of less self-quenching and high intensity over traditional Cy dyes under long-wavelength region [33]. In addition, KU dyes are newly developed fluorescent dyes that have long lifetime, it also has great potential in detection use.

As the aim of lifetime library is to be eventually used in biology detection and those fluorescent dyes have long been used as fluorescent probes, thus, in this part of work, nanoprobes that contain quantum dots and fluorescent dyes have been made.

5.2 Materials and Method

The fluorescent dyes that are used in this part of study includes Rhodamine (rhodamine) and Alexa Fluor 555 (AF 555) that both from ThermoFisher, and KU530 (KU) from KU Dyes.

In this part of study, 200 and 100μL of CZ are used. According to the information from vendor's webpage and previous experiments, we noticed that AF 555 is much brighter than rhodamine and KU, thus, 1, 3, 10, 30, 60 and 120μL of rhodamine and KU dyes were tested, 1, 3, 10, 30 and 60μL of AF 555 dyes were tested.

5.3 Characterization Results

5.3.1 Fluorescence Lifetime

As we mentioned before, 534nm excitation wavelength is more effective when analyzing probes that contains fluorescent dyes. Besides, as we also want to expand probe library be switch to other channels, phasor plots of the probes synthesized above were obtained under both 470nm and 534nm excitation wavelength.

470ex

(A1) CZ 200 + Rhodamine

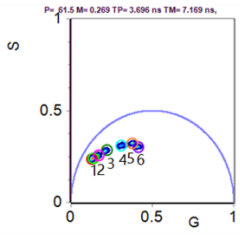

	Color	CZ (μL)	Rhodamine (μL)	DLS (nm)	Emission (470 ex, 590 nm)	Absorption (300 nm)	Emission / Absorption
1	Green	200	1	40.76	0.5345	0.6655	0.8031
2	Pink	200	3	43.04	0.5575	0.6108	0.9126
3	Dark Green	200	10	54.30	0.5375	0.7097	0.7573
4	Blue	200	30	42.78	0.3407	0.6496	0.5245
5	Orange	200	60	46.11	0.4239	0.7847	0.5402
6	Purple	200	120	37.49	0.4222	0.7484	0.5642

534ex

(A2) CZ 200 + Rhodamine

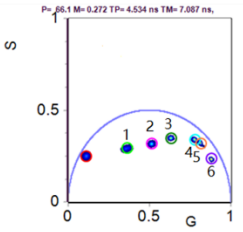

	Color	CZ (μL)	Rhodamine (μL)	DLS (nm)	Emission (534 ex, 590 nm)	Absorption (300 nm)	Emission / Absorption
1	Green	200	1	40.76	0.2207	0.6655	0.3316
2	Pink	200	3	43.04	0.2784	0.6108	0.4557
3	Dark Green	200	10	54.30	0.4043	0.7097	0.5697
4	Blue	200	30	42.78	0.5999	0.6496	0.9235
5	Orange	200	60	46.11	0.7229	0.7847	0.9212
6	Purple	200	120	37.49	0.6750	0.7484	0.9020

470ex

(A3) CZ 100 + Rhodamine

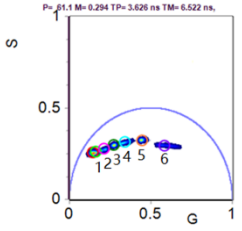

	Color	CZ (μL)	Rhodamine (μL)	DLS (nm)	Emission (470 ex, 590 nm)	Absorption (300 nm)	Emission / Absorption
1	Green	100	1	37.53	0.2252	0.3849	0.5850
2	Pink	100	3	61.21	0.0848	0.6206	0.1367
3	Dark Green	100	10	53.25	0.3022	0.4846	0.6235
4	Blue	100	30	66.32	0.2734	0.4677	0.5846
5	Orange	100	60	67.85	0.2045	0.4231	0.4834
6	Purple	100	120	51.61	0.1849	0.5333	0.3468

534ex

(A4) CZ 100 + Rhodamine

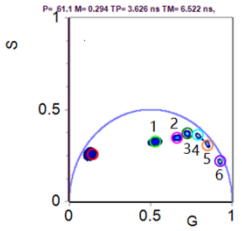

	Color	CZ (μL)	Rhodamine (μL)	DLS (nm)	Emission (534 ex, 590 nm)	Absorption (300 nm)	Emission / Absorption
1	Green	100	1	37.53	0.1037	0.3849	0.2695
2	Pink	100	3	61.21	0.1835	0.6206	0.2957
3	Dark Green	100	10	53.25	0.3793	0.4846	0.7826
4	Blue	100	30	66.32	0.6220	0.4677	1.3298
5	Orange	100	60	67.85	0.5931	0.4231	1.4018
6	Purple	100	120	51.61	0.5901	0.5333	1.1065

Figure 5.1 Characterization results of silica nanoparticle labeled with both CZ and rhodamine dyes ($3.4 \times 10^{-3}\ mol/L$): 200 μL CZ data measured under (A1) 470 and (A2) 534 nm excitation wavelength. 100 μL CZ data measured under (A3) 470 and (A4) 534 nm excitation wavelength. (Left) Fluorescence lifetime data. (Right) DLS results and intensity readings of emission and absorption of each probe.

470ex

(B1) CZ 200 + AF 555

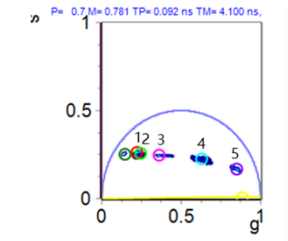

	Color	CZ (µL)	AF 555 (µL)	DLS (nm)	Emission (470 ex, 590 nm)	Absorption (300 nm)	Emission / Absorption
1	Red	200	1	38.47	0.4519	0.6685	0.6760
2	Green	200	3	35.08	0.7112	0.5912	1.2031
4	Pink	200	10	37.57	0.7696	0.5852	1.3151
5	Blue	200	30	32.08	0.6433	0.5735	1.1217
6	Purple	200	60	38.45	0.4949	0.6747	0.7335

534ex

(B2) CZ 200 + AF 555

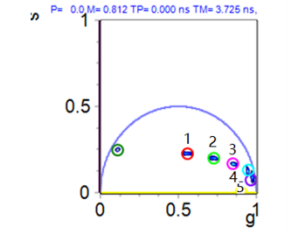

	Color	CZ (µL)	AF 555 (µL)	DLS (nm)	Emission (534 ex, 590 nm)	Absorption (300 nm)	Emission / Absorption
1	Red	200	1	38.47	0.0720	0.6685	0.1076
2	Green	200	3	35.08	0.1471	0.5912	0.2488
4	Pink	200	10	37.57	0.2703	0.5852	0.4618
5	Blue	200	30	32.08	0.4217	0.5735	0.7353
6	Purple	200	60	38.45	0.4534	0.6747	0.6720

470ex

(B3) CZ 100 + AF 555

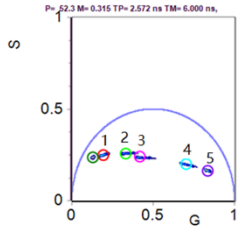

	Color	CZ (µL)	AF 555 (µL)	DLS (nm)	Emission (470 ex, 590 nm)	Absorption (300 nm)	Emission / Absorption
1	Red	100	1	34.77	0.3893	0.3676	1.0591
2	Green	100	3	34.55	0.1834	0.3535	0.5189
4	Pink	100	10	49.47	0.1379	0.4189	0.3292
5	Blue	100	30	46.26	0.3693	0.4344	0.8500
6	Purple	100	60	41.53	0.2984	0.4164	0.7166

534ex

(B4) CZ 100 + AF 555

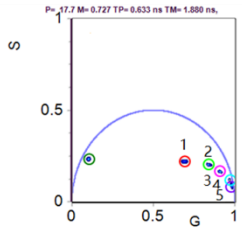

	Color	CZ (µL)	AF 555 (µL)	DLS (nm)	Emission (534 ex, 590 nm)	Absorption (300 nm)	Emission / Absorption
1	Red	100	1	34.77	0.0639	0.3676	0.1739
2	Green	100	3	34.55	0.0932	0.3535	0.2636
4	Pink	100	10	49.47	0.1827	0.4189	0.4362
5	Blue	100	30	46.26	0.3939	0.4344	0.9067
6	Purple	100	60	41.53	0.3821	0.4164	0.9176

Figure 5.2 Characterization results of silica nanoparticle labeled with both CZ and AF 555 dyes ($8.0 \times 10^{-3}\ mol/L$): 200 µL CZ data measured under (B1) 470 and (B2) 534 nm excitation wavelength. 100 µL CZ data measured under (B3) 470 and (B4) 534 nm excitation wavelength. (Left) Fluorescence lifetime data. (Right) DLS results and intensity readings of emission and absorption of each probe.

470ex

(C1) CZ 200 + KU

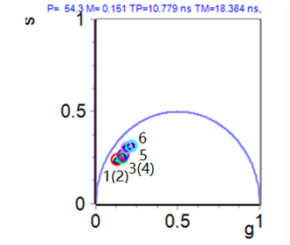

	Color	CZ (μL)	KU (μL)	DLS (nm)	Emission (470 ex, 590 nm)	Absorption (300 nm)	Emission / Absorption
1	Orange	200	1	37.53	0.2052	0.6581	0.3118
2	Yellow	200	3	61.21	0.1908	0.6527	0.2924
3	Green	200	10	53.25	0.2139	0.5492	0.3895
4	Purple	200	30	66.32	0.6207	0.7567	0.8202
5	Pink	200	60	67.85	0.2675	0.7177	0.3727
6	Blue	200	120	51.61	0.2711	0.7624	0.3556

534ex

(C2) CZ 200 + KU

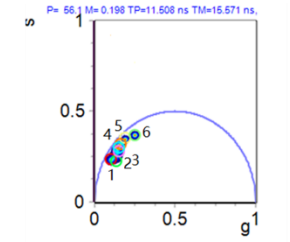

	Color	CZ (μL)	KU (μL)	DLS (nm)	Emission (534 ex, 590 nm)	Absorption (300 nm)	Emission / Absorption
1	Dark Green	200	1	38.48	0.1110	0.6581	0.1686
2	Pink	200	3	38.95	0.1209	0.6527	0.1853
3	Blue	200	10	35.67	0.1929	0.5492	0.3512
4	Orange	200	30	45.60	0.5152	0.7567	0.6809
5	Yellow	200	60	41.36	0.4737	0.7177	0.6601
6	Green	200	120	42.08	0.6028	0.7624	0.7906

470ex

(C3) CZ 100 + KU

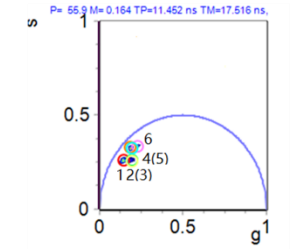

	Color	CZ (μL)	KU (μL)	DLS (nm)	Emission (534 ex, 590 nm)	Absorption (300 nm)	Emission / Absorption
1	Red	100	1	43.91	0.0885	0.3573	0.2477
2	Green	100	3	42.08	0.0852	0.3486	0.2443
3	Yellow	100	10	33.59	0.1259	0.3339	0.3770
4	Orange	100	30	48.89	0.1153	0.4463	0.2583
5	Blue	100	60	47.54	0.1607	0.4710	0.3411
6	Pink	100	120	47.23	0.1949	0.5591	0.3486

534ex

(C4) CZ 100 + KU

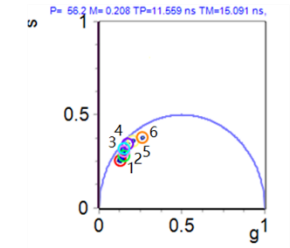

	Color	CZ (μL)	KU (μL)	DLS (nm)	Emission (470 ex, 590 nm)	Absorption (300 nm)	Emission / Absorption
1	Green	100	1	43.91	0.0517	0.3573	0.1448
2	Pink	100	3	42.08	0.0733	0.3486	0.2101
3	Blue	100	10	33.59	0.1458	0.3339	0.4366
4	Purple	100	30	48.89	0.3203	0.4463	0.7176
5	Yellow	100	60	47.54	0.4555	0.4710	0.9671
6	Orange	100	120	47.23	0.5854	0.5591	1.0470

Figure 5.3 Characterization results of silica nanoparticle labeled with both CZ and KU dyes ($4.1 \times 10^{-3}\ mol/L$): 200 μL CZ data measured under (C1) 470 and (C2) 534 nm excitation wavelength. 100 μL CZ data measured under (C3) 470 and (C4) 534 nm excitation wavelength. (Left) Fluorescence lifetime data. (Right) DLS results and intensity readings of emission and absorption of each probe.

From the fluorescent lifetime results about CZ with three kinds of dyes, rhodamine, AF 555 and KU, their fluorescence lifetime information can be acquired. However, under 470nm excitation wavelength, the lifetime of particles seems gathered together, this cannot achieve our goal of separate them with FLIM. When switch to 534nm wavelength, they can be separated on the phasor plot. This again shows that excite these particles under 534nm is more efficient.

Under 534nm, for particles that contains both CZ and rhodamines, with increased amount of rhodamine involved, at first, they locate on the line that connect 200 μL CZ and low amount of rhodamine. This kind of shifting is due to the linear combination that happened between quantum dots and fluorescent dyes. Then, as the concentration of dyes increased to 30 μL and more, their location on phasor goes down. Now, this phenomenon is more due to the quenching effect when the concentration of dye that used is high enough.

In the results of CZ with AF 555 and KU dyes, the situation above also occurs, while most of them follow the quenching trajectory as expected.

5.3.2 Fluorescent Analysis

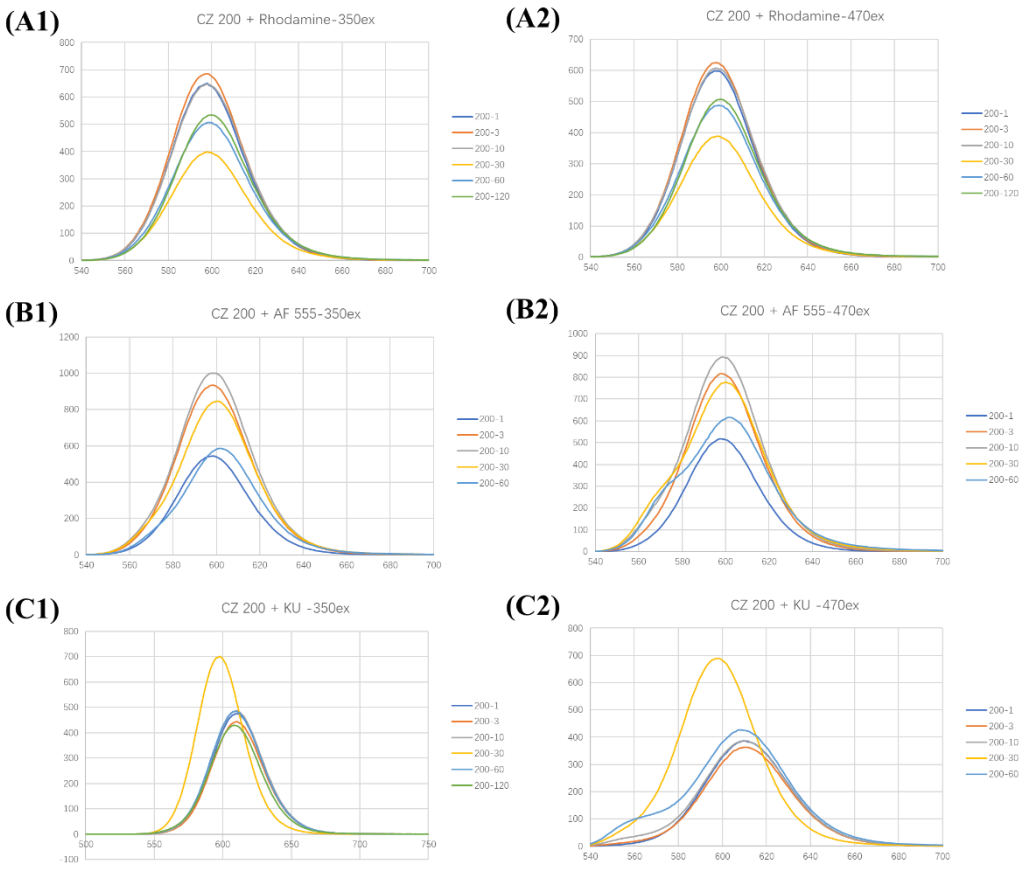

Figure 5.4: Emission spectra of 200 µL CZ with (A) rhodamine, (B) AF 555 and (C) KU under (1) 350 nm and (2) 470 nm excitation wavelength.

From emission spectra data, we can see that when probes were excited under 350nm and 470nm wavelength, emission wavelengths of CZ with rhodamine are very similar that shows up around 598nm. While for CZ with AF 555, there is a little bit red shift of the emission peaks to around 600nm. Then, when talking about CZ with KU dyes, a more obvious right shift appears, that the emission peaks shows up around 610nm. The red shift is a very interesting phenomenon as we do not see these happened when mixing quantum dots and dark quencher dyes. This might due to the reason that as more fluorescent dyes are incorporated, the concentration of polarized solute

increased, thus lead to the enhancement in solvent polarity [34].

Moreover, for all the CZ and dye mixtures, the change of emission intensity lack of regularity. When adding more rhodamine into the silica mesh, intensity first lower down and then goes up, whereas the situation for AF 555 and KU dyes is opposite, first goes up and then lower down. So, it puts up a question that the excitation wavelength we used may not be the most suitable one. According to the information from vendors' webpage and in order to make consistency with later FLIM detection, 534nm excitation wavelength was used when measuring probes that contains fluorescent dyes (as FLIM also provide 534ex channel).

	Ex	Em
CZ	——	585-600
Rhodamine	552	575
AF 555	555	572
KU	530	560

Figure 5.5: Generic excitation and emission wavelength for CZ, rhodamine, AF 555 and KU dyes from vendor's webpage.

After changing to 534nm excitation wavelength, spectra data shows interesting change. In the spectra of 200μL and 100μLCZ with rhodamine silica nanoprobes, as more fluorescent dyes are encapsulated, emission peaks gradually shifted from 598nm to around 585nm. From the results of CZ with AF 555, two peaks appear and the peak around 570nm becomes the mean peak and the peak around 605nm is shoulder peak. Besides, as amount of dyes are increased, the shoulder peak shows right shift from 600nm to 608nm. Results of CZ with KU dyes are similar with AF 555, as mean peak appears at 560nm and shoulder peak appears at 610nm. According to generic emission

wavelength that provided by vendors, peaks around 600nm is more about quantum dots dominated, thus, peaks appear between 560nm to 585nm is due to the fluorescent dyes dominated probes. This can explain the phenomenon that when increasing the amount of fluorescent dye, emission intensity of peak with smaller wavelength increases more than the other peak.

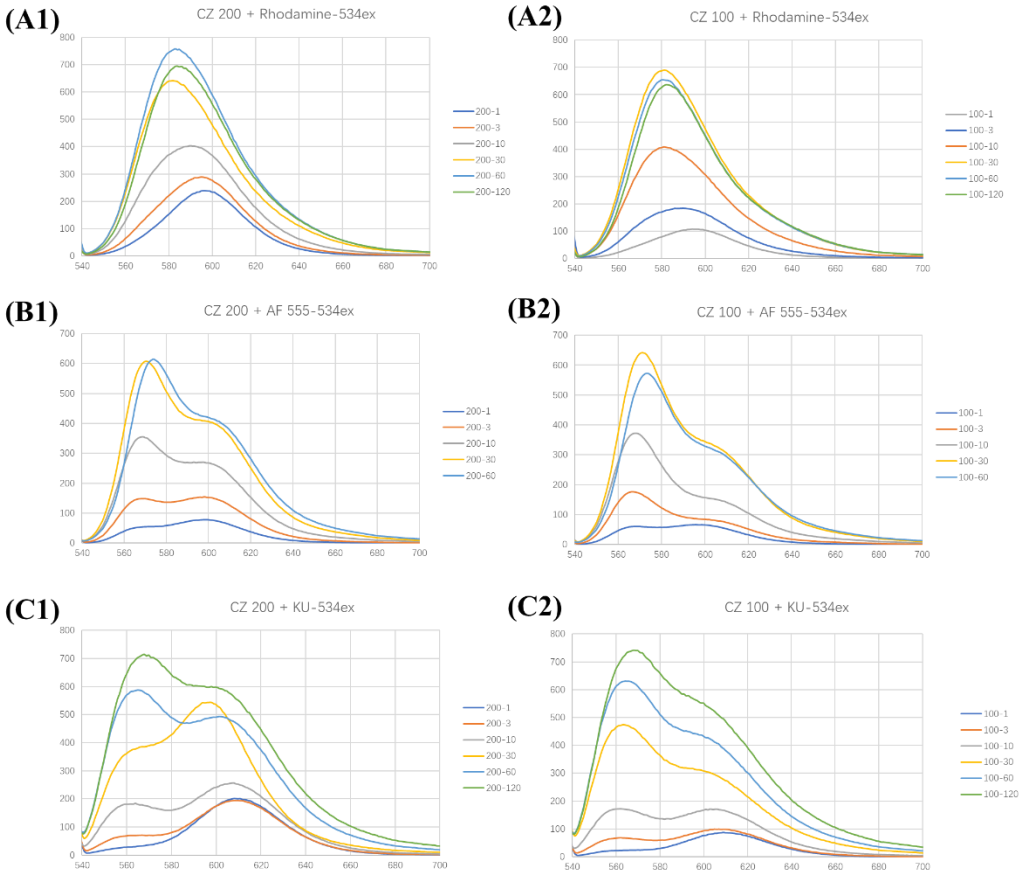

Figure 5.6: Emission spectra (1) 200 µL and (2) 100 µL CZ with (A) rhodamine, (B) AF 555 and (C) KU under 534 nm excitation wavelength.

Then from the fluorescence analysis data of these CZ and dye mixture, for increase amount used, absorption intensity and emission intensity are both increased. Moreover, emission intensity over

absorption intensity also show steady growth. This may due to the reason that while absorption intensities of all three kinds of dyes are increased, emission intensity increased more. This expected results really tell us that fluorescent dyes are truly been added into the silica mesh and at the meantime, interaction between quantum dot and fluorescent dye happened effectively.

All these data from fluorescence analysis provide a conclusion that it is very important to choose an appropriate excitation wavelength for better conducting fluorescence analysis. So, in this study, when characterizing probes that contain quantum dots and fluorescent dyes mixtures, best results can be obtained if 534nm excitation wavelength is employed.

5.3.3 Size

Diameter range of silica nanoparticles with CZ and rhodamine combination are between 39nm to 70nm, average size is around 45nm. While for CZ and AF 555 probes, nanoparticle have the average diameter of 40nm, ranged from 30 to 51nm. Average particle size of CZ and KU combination are around 40nm, ranged from 33 to 48nm in diameter. With more dyes are employed, the size of particles gradually increased. Overall size of CZ and fluorescent dyes nanoprobes are around 30 to 50nm, which shows particles are uniformly synthesized.

5.4 Fluorescent Lifetime Nanoprobe Library in this Chapter

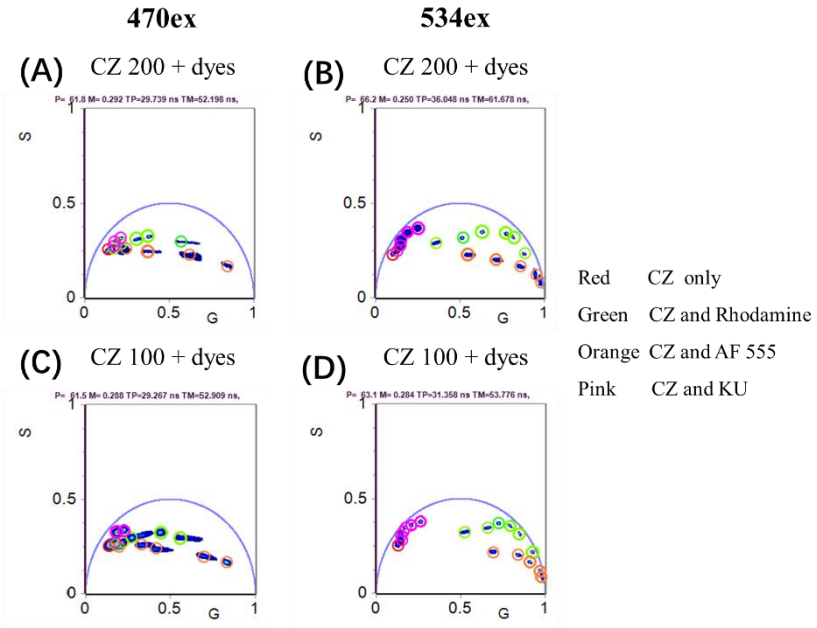

Figure 5.7 Global fluorescent lifetime results of silica nanoparticles that labeled with CZ and three kinds of fluorescent dyes: rhodamine, AF 555 and KU. (A) 200 μL CZ with various amount of dyes under 470 nm and (B) 534 nm excitation wavelength. (C) 100 μL CZ with various amount of dyes under 470 nm and (D) 534 nm excitation wavelength.

Chapter 6 Summary

With the desire to treat cancer more efficiently, key cell types should first be identified. The existing analysis methods have many limitations thus they cannot currently provide enough molecular information. The phasor approach to FLIM shows its potential as the fluorescent lifetime information of probes can be directly presented on a phasor plot. However, the lack of detection channels makes it difficult to use in the real world. Thus, the urgent task is to enlarge the detection channels and gathered them into a library for future use.

Three kinds of fluorescent lifetime nanoprobe libraries have been constructed. The first is made by silica nanoprobes with three quantum dot species, CZ, CIS and Strem. The second one is built by employing four kinds of quantum dots, but with various amount of dark quencher dyes. The third library is constructed by encapsulating CZ with fluorescent dyes, rhodamine, AF 555 and KU dyes.

DLS results show that the diameter of probes is in a range from 30 to 50 nm, which means that they have been uniformly made. Fluorescent analysis results help to characterize the nanoprobes qualitatively and quantitatively. Absorption data clearly shows that silica nanoparticles have been made successfully and all fluorescent species are effectively encapsulated inside the silica nanoparticles. Emission data matches with theoretical the quenching effect occurred between the two fluorescent species. As more dark quencher dyes are involved in the nanoprobe synthesis

process, emission intensity is weakened. With more fluorescent dyes used, overall emission intensity is strengthened. Overall fluorescent intensity results that have been calculated by emission intensity/absorption intensity verified the theoretical photon emission efficiency as the quantities of fluorescent species changes.

The phasor plot obtained by FLIM shows fluorescent lifetime results. Even though the fluorescent species have similar emission wavelengths, they can occupy different places on the phasor plot. By mixing different species and changing the amount added, the goal to manipulating their lifetimes can be achieved. Thus, the probe libraries with tunable fluorescent lifetime are constructed with three types of fluorescent species: quantum dots, dark quencher dyes, and fluorescent dyes. These results all match the fluorescence analysis. According to the FLIM results of the quantum dots with fluorescent dyes, additional spectral window, 534nm excitation, has been developed beyond the traditional 470nm excitation window. This shows the feasibility of expanding the libraries to more spectral windows.

All in all, the whole study has successfully constructed three kinds of fluorescent lifetime probe mixtures through the interaction between quantum dots, dark quencher dyes and fluorescent dyes. While changing the ratio of fluorescent species encapsulated inside the silica nanoparticles, probe lifetimes become tunable. This provides the potential to enlarging the probe lifetime libraries.

One of the primary tasks for future research is to find new fluorescent species with unique lifetimes

in order to fill more spots on the phasor plot. In addition, expanding the spectral detection windows is another central goal. This could enhance applicability and commonality of our lifetime nanoprobe libraries for future practical use. On the other hand, with the exiting probes, it will be meaningful to study the quenching effect in order to fill the phasor plot with fewer fluorescent species, which can simplify the synthesis process while still retaining the efficiency of tumor detection.

Bibliography

[1] Cronin, K. A., Lake, A. J., Scott, S., Sherman, R. L., Noone, A. M., Howlader, N., ... & Kohler, B. A. (2018). Annual Report to the Nation on the Status of Cancer, part I: National cancer statistics. *Cancer*, *124*(13), 2785-2800.

[2] Rahim, M. K. (2017). *Sensitive, multiplexed molecular profiling with nanomaterial probes for cancer diagnostics* (Doctoral dissertation, UC Irvine).

[3] Lin, M. T. , Mosier, S. L. , Thiess, M. , Beierl, K. F. , Debeljak, M. , & Tseng, L. H. , et al. (2014). Clinical validation of kras, braf, and egfr mutation detection using next-generation sequencing. *American Journal of Clinical Pathology, 141*(6), 856-866.

[4] Fuhr, J. E. , Frye, A. , Kattine, A. A. , & Meter, S. V. . (1991). Flow cytometric determination of breast tumor heterogeneity. *Cancer, 67*(5), 1401-1405.

[5] Xu, X., Li, H., Hasan, D., Ruoff, R. S., Wang, A. X., & Fan, D. L. (2013). Near-field enhanced plasmonic-magnetic bifunctional nanotubes for single cell bioanalysis. *Advanced Functional Materials, 23*(35), 4332-4338.

[6] Schlücker, S. (2009). SERS microscopy: nanoparticle probes and biomedical applications. *ChemPhysChem*, *10*(9-10), 1344-1354.

[7] Bandura, D. R., Baranov, V. I., Ornatsky, O. I., Antonov, A., Kinach, R., Lou, X., ... & Tanner, S. D. (2009). Mass cytometry: technique for real time single cell multitarget immunoassay based on inductively coupled plasma time-of-flight mass spectrometry. Analytical chemistry, 81(16), 6813-6822.

[8] Yoshio, S. , & Kenji, Y. . (2015). Development of functional fluorescent molecular probes for the detection of biological substances. Biosensors, 5(2), 337-363.

[9] Oida, T., Sako, Y., & Kusumi, A. (1993). Fluorescence lifetime imaging microscopy (flimscopy). methodology development and application to studies of endosome fusion in single cells. *Biophysical Journal, 64*(3), 676-685.

[10] Bastiaens, P. I. H. , & Squire, A. . (1999). Fluorescence lifetime imaging microscopy: spatial resolution of biochemical processes in the cell. *Trends in Cell Biology, 9*(2), 48-52.

[11] Digman, M. A. , Caiolfa, V. R. , Zamai, M. , & Gratton, E. . (2008). The phasor approach to fluorescence lifetime imaging analysis. *Biophysical Journal, 94*(2), L14-L16.

[12] Liao, S. C., Sun, Y., & Coskun, U. (2015). FLIM Analysis using the Phasor Plots.

[13] Mohanraj, V. J., and Chen, Y. (2006). Nanoparticles—a review. *Tropic Journal of Pharmaceutical Research*, 5(1), 561–573.

[14] Arap, W. , Pasqualini, R. , Montalti, M. , Petrizza, L. , Prodi, L. , & Rampazzo, E. , et al. (2013). Luminescent silica nanoparticles for cancer diagnosis. Current Medicinal Chemistry,

20(17), 2195-2211.

[15] Lin, J., Chen, H., Yan, J., & Yu, Z. (2012). Functionally modified monodisperse core–shell silica nanoparticles: silane coupling agent as capping and size tuning agent. *Colloids & Surfaces A Physicochemical & Engineering Aspects, 411*(411), 111-121.

[16] Mader, H. , Li, X. , Saleh, S. , Link, M. , & Wolfbeis, O. S. . (2008). Fluorescent silica nanoparticles. *Annals of the New York Academy of Sciences, 1130*(1), 218-223.

[17] Ow, H. , Larson, D. R. , Srivastava, M. , Baird, B. A. , & Wiesner, U. . (2005). Bright and stable core−shell fluorescent silica nanoparticles. *Nano Letters, 5*(1), 113-117.

[18] Hu, Z., Tan, J., Lai, Z., Rong, Z., Zhong, J., & Wang, Y., et al. (2017). Aptamer combined with fluorescent silica nanoparticles for detection of hepatoma cells. Nanoscale Research Letters, 12(1), 96.

[19] Zhao, X. J. , Bagwe, R. A. P. , & Tan, W. H. . (2004). Development of organic-dye-doped silica nanoparticles in a reverse microemulsion. Advanced Materials, 16(2), 173-176.

[20] Santra, S. , Zhang, P. , Wang, K. , Tapec, R. , & Tan, W. . (2001). Conjugation of biomolecules with luminophore-doped silica nanoparticles for photostable biomarkers. Analytical Chemistry, 73(20), 4988-4993.

[21] Lin, Y. S., Wu, S. H., Tseng, C. T., Hung, Y., Chang, C., and Mou. C. Y. (2009). Synthesis of hollow silica nanospheres with a microemulsion as the template. Chemical Communications, 2009(24):3542-3544.

[22] Rochira, J. A., Gudheti, M. V., Gould, T. J., Laughlin, R. R., Nadeau, J. L., & Hess, S. T. (2007). Fluorescence intermittency limits brightness in CdSe/ZnS nanoparticles quantified by fluorescence correlation spectroscopy. The Journal of Physical Chemistry C, 111(4), 1695-1708.

[23] Zhou, C., Yuan, H., Shen, H., Guo, Y., Li, X., & Liu, D., et al. (2011). Synthesis of size-tunable photoluminescent aqueous cdse/zns microspheres via a phase transfer method with amphiphilic oligomer and their application for detection of hcg antigen. Journal of Materials Chemistry, 21(20), 7393-7400.

[24] Medintz, I. L. , Uyeda, H. T. , Goldman, E. R. , & Mattoussi, H. . (2005). Quantum dot bioconjugates for imaging, labelling and sensing. Nature Materials, 4(6), 435-446.

[25] Sapsford, K. E., Pons, T., Medintz, I. L., Higashiya, S., Brunel, F. M., Dawson, P. E., & Mattoussi, H. (2007). Kinetics of metal-affinity driven self-assembly between proteins or peptides and CdSe− ZnS quantum dots. The Journal of Physical Chemistry C, 111(31), 11528-11538.

[26] Boeneman, K., Mei, B. C., Dennis, A. M., Bao, G., Deschamps, J. R., & Mattoussi, H., et al. (2009). Sensing caspase 3 activity with quantum dot-fluorescent protein assemblies. Journal of the American Chemical Society, 131(11), 3828-9.

[27] Pons, T., Medintz, I., Sykora, M., & Mattoussi, H. (2006). Spectrally resolved energy transfer using quantum dot donors: Ensemble and single-molecule photoluminescence studies. Physical Review B, 73(24).

[28] Chou, K., F., and Dennis, A., M. (2015). Forster resonance energy transfer between quantum dot donors and quantum dot acceptors. Sensors, 15(6):13288—13325.

[29] Le Reste, L., Hohlbein, J., Gryte, K., & Kapanidis, A. N. (2012). Characterization of dark quencher chromophores as nonfluorescent acceptors for single-molecule FRET. *Biophysical journal*, *102*(11), 2658-2668.

[30] Chevalier, A., Massif, C., Renard, P. Y., & Romieu, A. (2013). Bioconjugatable Azo-Based Dark-Quencher Dyes: Synthesis and Application to Protease-Activatable Far-Red Fluorescent Probes. Chemistry–A European Journal, 19(5), 1686-1699.

[31] Christie, R. M. . (1993). Fluorescent dyes. Review of Progress in Coloration and Related Topics, 1(23), 1-18.

[32] Kenmoku, S. , Urano, Y. , Kojima, H. , & Nagano, T. . (2007). Development of a highly specific rhodamine-based fluorescence probe for hypochlorous acid and its application to real-time imaging of phagocytosis. Journal of the American Chemical Society, 129(23), 7313-7318.

[33] Berlier, J. E. , Rothe, A. , Buller, G. , Bradford, J. , Gray, D. R. , & Filanoski, B. J. , et al. (2003). Quantitative comparison of long-wavelength alexa fluor dyes to cy dyes: fluorescence of the dyes and their bioconjugates. Journal of Histochemistry & Cytochemistry, 51(12), 1699-1712.

[34] Zhang, X., Liu, M., Yang, B., Zhang, X., Chi, Z., Liu, S., ... & Wei, Y. (2013). Cross-linkable aggregation induced emission dye based red fluorescent organic nanoparticles and their cell imaging applications. Polymer Chemistry, 4(19), 5060-5064.